◆ Human Brain Mapping 36:2809–2825 (2015) ◆

Connectivity-Based Parcellation of the Thalamus in Multiple Sclerosis and Its Implications for Cognitive Impairment: A Multicenter Study

Alvino Bisecco,[1,2,3] Maria A. Rocca,[1,4] Elisabetta Pagani,[1] Laura Mancini,[5] Christian Enzinger,[6] Antonio Gallo,[2,3] Hugo Vrenken,[7] Maria Laura Stromillo,[8] Massimiliano Copetti,[1] David L. Thomas,[9] Franz Fazekas,[6] Gioacchino Tedeschi,[2,3] Frederik Barkhof,[7] Nicola De Stefano,[8] Massimo Filippi,[1,4]* and MAGNIMS Network

[1]*Neuroimaging Research Unit, Institute of Experimental Neurology, Division of Neuroscience, San Raffaele Scientific Institute, Vita-Salute San Raffaele University, Milan, Italy*
[2]*I Division of Neurology, Department of Medical, Surgical, Neurological, Metabolic and Aging Sciences, Second University of Naples, Naples, Italy*
[3]*MRI Center "SUN-FISM," Second University of Naples and Institute of Diagnosis and Care "Hermitage-Capodimonte," Naples, Italy*
[4]*Department of Neurology, Institute of Experimental Neurology, Division of Neuroscience, San Raffaele Scientific Institute, Vita-Salute San Raffaele University, Milan, Italy*
[5]*National Hospital for Neurology and Neurosurgery, UCLH NHS Foundation Trust, London, UK*

Contract grant sponsor: Italian Ministry of Health; Contract grant number: GR-2009–1529671; Contract grant sponsor: Fondazione Italiana Sclerosi Multipla; Contract grant number: FISM2011/R19; Contract grant sponsor: Dutch MS Research Foundation (MS Center Amsterdam); Contract grant number: 09–538d; Contract grant sponsor: MAGNIMS-ECTRIMS Fellowship (Dr. Bisecco)

*Correspondence to: Massimo Filippi; Neuroimaging Research Unit, Institute of Experimental Neurology, Division of Neuroscience, San Raffaele Scientific Institute, Vita-Salute San Raffaele University, Via Olgettina, 60, 20132 Milan, Italy.
E-mail: filippi.massimo@hsr.it

Conflicts of interest: Dr. Rocca received speakers honoraria from Novartis and Serono Symposia International Foundation and receives research support from the Italian Ministry of Health and Fondazione Italiana Sclerosi Multipla. Drs Bisecco, Pagani, Mancini, Enzinger, Stromillo, Copetti, Thomas and Vrenken have nothing to disclose. Dr. Gallo received honoraria for speaking and travel grants from Biogen, Sanofi-Aventis, Merck Serono, Genzyme, Teva, Bayer-Schering and Novartis. Prof. Fazekas serves on scientific advisory boards for Bayer Schering, Biogen Idec, Genzyme, Merck Serono, Pfizer, Novartis and Teva Pharmaceutical Industries Ltd.; performs reading services for Parexel; and has received speaker honoraria and support from Biogen Idec, Bayer Schering, Merck Serono, Novartis, Sanofi-Aventis and Teva Pharmaceutical Industries Ltd. Prof. Barkhof serves/has served on the advisory boards of Bayer-Schering Pharma, Sanofi-Aventis, Biogen Idec, UCB, Merck-Serono, Novartis, and Roche. He received funding from the Dutch MS Society and has been a speaker at symposia organized by the Serono Symposia Foundation. Prof. Tedeschi has received speaker honoraria from Sanofi-Aventis, Merck Serono, Bayer Schering Pharma, Novartis, and Biogen-Idec; and has received funding for travel from Bayer Schering Pharma, Biogen-Idec, Merck Serono, Novartis, and Sanofi Aventis. Prof. De Stefano has served on scientific advisory boards and steering committees of clinical trials for Merck Serono SA, Teva, and Novartis Pharma AG, and has received support for congress participation or speaker honoraria from Biogen Idec, Merck Serono S.A., Bayer-Schering AG, Teva, Sanofi-Aventis, and Novartis Pharma AG. He received grants from the Italian MS Society, outside the submitted work. Prof Filippi serves on scientific advisory boards for Teva Pharmaceutical Industries; has received compensation for consulting services and/or speaking activities from Bayer Schering Pharma, Biogen Idec, Merck Serono, and Teva Pharmaceutical Industries; and receives research support from Bayer Schering Pharma, Biogen Idec, Merck Serono, Teva Pharmaceutical Industries, Italian Ministry of Health, Fondazione Italiana Sclerosi Multipla, Cure PSP, and the Jacques and Gloria Gossweiler Foundation (Switzerland).

Revised 25 February 2015; Accepted 25 March 2015.
DOI: 10.1002/hbm.22809
Published online 14 April 2015 in Wiley Online Library (wileyonlinelibrary.com).

[6]Department of Neurology, Medical University of Graz, Austria
[7]Department of Radiology and Nuclear Medicine, MS Centre Amsterdam, VU University Medical Centre, Amsterdam, The Netherlands
[8]Department of Neurological and Behavioral Sciences, University of Siena, Italy
[9]Neuroradiological Academic Unit, UCL Institute of Neurology, Queen Square, London, United Kingdom

Abstract: In this multicenter study, we performed a tractography-based parcellation of the thalamus and its white matter connections to investigate the relationship between thalamic connectivity abnormalities and cognitive impairment in multiple sclerosis (MS). Dual-echo, morphological and diffusion tensor (DT) magnetic resonance imaging (MRI) scans were collected from 52 relapsing-remitting MS patients and 57 healthy controls from six European centers. Patients underwent an extensive neuropsychological assessment. Thalamic connectivity defined regions (CDRs) were segmented based on their cortical connectivity using diffusion tractography-based parcellation. Between-group differences of CDRs and cortico-thalamic tracts DT MRI indices were assessed. A vertex analysis of thalamic shape was also performed. A random forest analysis was run to identify the best imaging predictor of global cognitive impairment and deficits of specific cognitive domains. Twenty-two (43%) MS patients were cognitively impaired (CI). Compared to cognitively preserved, CI MS patients had increased fractional anisotropy of frontal, motor, postcentral and occipital connected CDRs ($0.002<P<0.02$). They also experienced more pronounced atrophy in anterior thalamic regions and abnormal DT MRI indices of all cortico-thalamic tracts. Damage of specific cortico-thalamic tracts explained global cognitive dysfunction and impairment of selected cognitive domains better than all other MRI variables. Thalamic CDR DT MRI abnormalities were correlated with abnormalities of the corresponding cortico-thalamic tracts. Cortico-thalamic disconnection is, at various levels, implicated in cognitive dysfunction in MS. Thalamic involvement in CI MS patients is likely related to gray matter rather than white matter damage of thalamic subregions. *Hum Brain Mapp 36:2809–2825, 2015.*

Key words: multiple sclerosis; DT MRI; cognitive impairment; thalamus; gray matter; white matter

INTRODUCTION

The thalamus is a relay and integration center connecting subcortical and cortical regions, which plays a crucial role in CNS function, being responsible for awareness, sensory, motor, and cognitive functions [Johnson and Ojemann, 2000]. Pathological and imaging studies have consistently detected a high vulnerability to damage of this strategic gray matter (GM) structure in multiple sclerosis (MS) patients from the earliest stages of the disease [Henry et al., 2008]. MS-related thalamic involvement is clinically relevant, since it has been correlated not only to the severity and progression of clinical disability, but also to cognitive dysfunction [Minagar et al., 2013].

Using advanced magnetic resonance imaging (MRI) techniques, a number of studies has shown that thalamic atrophy is the most significant MRI correlate of cognitive impairment both in adult [Batista et al., 2012; Benedict et al., 2006; Benedict et al., 2004; Houtchens et al., 2007] and pediatric [Till et al., 2011] patients with MS. Other factors which have been analyzed to explain the role of the thalamus for cognitive deficits in MS include the presence of diffuse microstructural damage preceding the development of tissue loss and functional alterations of this relay station. In this regard, poor cognitive performance has been related to thalamic diffusion tensor (DT) MRI abnormalities [Benedict et al., 2013; Tovar-Moll et al., 2009] and to increased thalamocortical resting state functional connectivity [Tona et al., 2014].

The thalamus is an extremely complex structure, organized in nuclear groups with specific functions and connections with cortical and subcortical areas. This is why the study of the whole thalamus could be inadequate to explain deficits of specific functions, as suggested by a recent shape analysis study which found an association between atrophy of the thalamic ventral nuclear complex and disability [Magon et al., 2014]. To our knowledge, the relationship between regional thalamic damage and cognitive impairment in MS has not been investigated, yet.

TABLE I. Main demographic, clinical, and conventional MRI characteristics of patients with MS and HC enrolled in this study at six European centers

	Amsterdam		Graz		London		Milan		Naples		Siena		
Group	HC	MS	HC	MS	HC	MS	HC	MS	HC	MS	HC	MS	*P*
M/W	3/6	4/4	8/3	5/1	4/5	3/4	4/6	3/7	3/5	3/8	2/8	1/9	0.01[b]
Mean age (SD) (years)	45.2 (6.7)	49.4 (4.6)	34.2 (6.4)	37.2 (10.2)	32.2 (5.1)	39.4 (9.8)	33.8 (8.2)	37.4 (8.3)	34.8 (10.5)	38.8 (7.8)	39.7 (12.5)	39.8 (6.2)	<0.001[a]
Median EDSS (range)	—	3.5 (2.0–4.0)	—	2.5 (0–4)	—	2.0 (1.0–4.0)	—	1.5 (1.5–4.0)	—	1.5 (1.0–6.0)	—	1.5 (1.0–4.0)	0.007[a]
Mean disease duration (SD) (years)	—	7.4 (4.5)	—	8.9 (7.3)	—	4.4 (2.5)	—	7.4 (9.1)	—	12.4 (7.9)	—	8.1 (4.4)	n.s.[a]
CP/CI patients	—	4/4	—	4/2	—	3/4	—	4/6	—	5/6	—	9/1	n.s.[b]
Mean T2 LV (SD) (ml)	—	11.9 (11.7)	—	23.1 (23.5)	—	16.9 (22.9)	—	8.9 (8.6)	—	6.9 (5.7)	—	5.3 (5.9)	n.s.[a]
Mean T1 LV (SD) (ml)	—	6.3 (7.4)	—	10.0 (10.1)	—	6.6 (7.0)	—	4.6 (4.5)	—	6.2 (4.9)	—	2.7 (3.0)	n.s.[a]
Mean NBV (SD) [ml]	1530 (49)	1394 (120)	1552 (79)	1479 (170)	1601 (76)	1521 (118)	1493 (67)	1444 (85)	1536 (60)	1402 (96)	1452 (67)	1370 (67)	<0.001[a]
Mean NGMV (SD) (ml)	818 (29)	754 (49)	838 (55)	792 (131)	876 (47)	808 (88)	789 (45)	778 (65)	844 (37)	786 (51)	779 (58)	752 (40)	0.003[a]
Mean NWMV (SD) (ml)	711 (38)	640 (76)	714 (35)	686 (75)	725 (49)	713 (62)	704 (35)	666 (81)	692 (45)	616 (54)	674 (34)	618 (36)	<0.001[a]

[a]Kruskal-Wallis test for site heterogeneity.
[b]Chi-Square test.
SD, standard deviation; M, men; W, women; HC, healthy controls; MS, multiple sclerosis; EDSS, Expanded Disability Status scale; CP, cognitively preserved; CI, cognitively impaired; LV, lesion volume; NBV, normalized brain volume; NGMV, normalized gray matter volume; NWMV, normalized white matter volume.

Integration of DT tractography with high-resolution T1 structural anatomical imaging has allowed a connectivity-based parcellation of the thalamic subregions and tracing their connections with the cortex [Behrens et al., 2003a]. The application of this technique to a large cohort of healthy subjects has provided robust correlation between regional thalamic volumes and tract characteristics with cognitive performance [Philp et al., 2014].

To shed light on the link between thalamic damage and neuropsychological involvement in MS patients, in this multicenter study, we applied the aforementioned approach to investigate the relation between abnormalities of regional thalamic MRI measures and connectivity versus cognitive performance. Our working hypothesis was that deficits of selected cognitive domains may be linked to damage of specific thalamic subregions and/or thalamo-cortical connections.

METHODS

Subjects

Subjects were recruited at six European centers (www.magnims.eu), which included: (a) the Department of Radiology, VU University Medical Centre, Amsterdam (Netherlands); (b) the Research Unit for Neuronal Repair and Plasticity, Medical University Graz, Graz (Austria); (c) the Queen Square MS Imaging Centre, University College London Institute of Neurology, London (UK); (d) the Neuroimaging Research Unit, "Vita-Salute" University, San Raffaele Scientific Institute, Milan (Italy); (e) the MRI Center "SUN-FISM", Second University of Naples, Naples (Italy); and (f) the Department of Neurological and Behavioral Sciences, University of Siena (Italy).

The inclusion criteria for this study required all subjects to be right-handed [Oldfield, 1971] and aged between 20 and 65 years. In addition, patients had to have a diagnosis of relapsing remitting (RR) MS [Lublin and Reingold, 1996; Polman et al., 2011], and no relapse or corticosteroid treatment within the month prior to scanning.

One patient and one healthy control (HC) had to be excluded from the final analysis because they did not complete the scanning protocol.

The final dataset used for this analysis included 52 RRMS patients (19/33 men/women; mean age=40.3 years, standard deviation (SD)=8.5 years, range=21–56 years; mean disease duration=8.4 years, range=2–33 years; median Expanded Disability Status Scale (EDSS) score=2.0, range=0.0–6.0) and 57 HC (24/33 men/women, mean age=36.6 years, SD=9.3 years, range=22–65 years). Table I shows the main demographic and clinical characteristics of the study subjects divided per site. Sex did not differ significantly between HCs and MS patients ($P=0.6$), whereas HCs were significantly younger than MS patients ($P=0.03$).

Local ethics approval was obtained at all sites and all subjects gave written informed consent.

Clinical and Neuropsychological Assessment

Within 48 h from the MRI acquisition, MS patients underwent a neurological evaluation with rating of the EDSS score and a neuropsychological assessment, performed at each participating site by an experienced neurologist and neuropsychologist, unaware of the MRI results, using validated translations of the neuropsychological tests. Cognitive performance was assessed using the Brief Repeatable Battery of Neuropsychological Tests (BRB-N) [Rao et al., 1991], only marginally influenced by language or cultural differences [Sepulcre et al., 2006]. BRB-N includes the Selective Reminding Test (SRT) to assess verbal memory; the 10/36 Spatial Recall Test (10/36 SRT) to assess visual memory; the Symbol Digit Modalities Test and the Paced Auditory Serial Addition Test 2″ and 3″ [Gronwall, 1977] to assess attention and information processing speed; and the Word List Generation test to assess verbal fluency. As previously described [Rocca et al., 2014; Sepulcre et al., 2006], Z-scores for each of the previous domains and a global Z-score of cognitive function (obtained by averaging Z-scores of all tests) were calculated.

In addition, the Wisconsin Card Sorting Test (WCST) was administered to evaluate executive functions [Heaton, 1993]. Performance at the WCST was evaluated by computing scores related to the total errors (WCSTte), the number of perseverative errors (WCSTpe), and the number of perseverative responses (WCSTpr) [Heaton, 1993]. Patients with a score $\leq$2 SD in at least one of these measures were considered impaired at the WCST [Filippi et al., 2012; Mattioli et al., 2010; Parisi et al., 2014].

Patients with at least two abnormal tests (defined as a score more than 2 SDs below the normative value provided by Boringa et al. [2001] for the BRB-N and by Heaton et al. [1993] for the WCST) were considered cognitively impaired (CI) [Lazeron et al., 2005; Portaccio et al., 2009].

MRI Acquisition

Brain MRI scans were obtained using magnets operating at 3.0 Tesla at all sites (Amsterdam and Naples: GE Signa; Graz and London: Siemens Trio; Milan and Siena: Philips Intera). In all subjects, the following sequences of the brain were collected during a single session: (a) pulsed gradient spin echo (PGSE) [Stejskal, 1965] single-shot-echo planar imaging (SS-EPI) sequence with a double-refocused variant [Reese et al., 2003] on Siemens and GE scanners to minimize eddy-current distortions, and single-echo EPI acquisition on Philips scanners. The following target scan parameters were used: repetition time (TR): 6,000–12,000 ms; echo time (TE): 70–100 ms, field of view (FOV): 320 $\times$ 240 mm^2; acquisition matrix: 128 $\times$ 96, 50 slices with an isotropic resolution (cubic voxels) of 2.5 mm; phase encoding direction: anterior-posterior. Thirty diffusion weighted (DW) volumes [Jones, 2004] were acquired, each with a different diffusion encoding gradient vector direction, and with a constant *b*-factor of 900 s/mm^2. For one of the two Siemens scanners where it was not possible to use 30 directions because of pulse sequence limitations, the maximum number available (=12) was used, with an increased number of repetitions such that the product of the number of DW directions and the number of repetitions was kept close to 30. Four sites acquired four b0 images, while the remaining two sites acquired two b0 images. Parallel acquisition with an acceleration factor=2 was used [Pagani et al., 2010]. In addition, five repetitions of the b0 image were acquired from one HC per center, to allow signal-to-noise ratio (SNR) estimation. (b) Dual-echo turbo-spin-echo (TSE): TR=ranging from 4,000 to 5,380 ms, TE_1=ranging from 10 to 23 ms, TE_2=ranging from 90 to 102 ms, echo train length =ranging from 5 to 11, 44 contiguous, 3-mm thick axial slices, parallel to the AC-PC plane, with a matrix size=256 $\times$ 192 and a FOV= 240 $\times$ 180 mm^2 (recFOV=75%) and (c) 3D T1-weighted scan: TR=ranging from 5.5 to 8.3 ms (for GE/Philips scanners) and from 1,900 to 2,300 ms (for Siemens scanners); TE=ranging from 1.7 to 3.0 ms; flip angle ranging from 8°–12°, 176–192 sagittal slices with thickness=1 mm and in-plane resolution=1 $\times$ 1 mm^2. Geometric distortions caused by the nonlinearity of the imaging field gradients were corrected on 3D T1 weighted scans (2D correction for Siemens and GE scanners and 3D correction for Philips).

Conventional MRI Analysis

The analysis of structural MRI data was done centrally at the Neuroimaging Research Unit (Milan, Italy) by experienced observers, unaware of subject identity. T2 hyperintense and T1 hypointense lesion volumes (LV) were measured on dual-echo TSE and 3D T1-weighted scans, respectively, using a local thresholding segmentation technique (Jim 5.0, Xinapse Systems, West Bergholt, UK). Normalized brain (NBV), WM (NWMV) and GM (NGMV) volumes were measured on 3D T1-weighted scans using the SIENAx software [Smith et al., 2002], after T1-hypointense lesion refilling [Chard et al., 2010].

SNR Calculation

SNR was calculated using five repeated acquisitions of the b0 image and determined as the ratio of the temporal mean value to the SD, averaged within a region of interest positioned in a uniform WM area. This method is the most accurate when multichannel coils are used and the assumption of homogeneous background noise cannot be satisfied [Dietrich et al., 2007].

Connectivity-Based Parcellation of the Thalami

Preprocessing

DW images were first corrected for distortions caused by the eddy currents and for movements (http://white.stanford.edu/newlm/index.php/DTI_Preprocessing). Then, using the FMRIB's Diffusion Toolbox (FDT tool, FSL 5.0.5, http://www.fmrib.ox.ac.uk), the DT was estimated in each voxel by linear regression [Basser et al., 1994] and fractional anisotropy (FA) and mean diffusivity (MD) maps were derived. DW data were modeled with 2 fibers per voxel and distributions of diffusion parameters were derived (BEDPOSTX Tool in FSL). This step creates the input files necessary for running probabilistic tractography [Behrens et al., 2007; Behrens et al., 2003b]. The following steps are required to relate the b0 image space to MNI space, where cortical lobes are defined. To compensate for susceptibility induced distortions that particularly affect DW data acquired with an EPI read-out, the T2-weighted TSE image was used as a reference image for nonlinear registration. After skull stripping using the brain extraction tool (BET) (fsl.fmrib.ox.ac.uk/fsl/fslwiki/BET) [Smith, 2002], the T2-weighted image was rigidly aligned to the b0 EPI image [Jenkinson and Smith, 2001]. Then, a nonlinear deformation of the b0 image was applied so that it matched the registered T2-weighted TSE compensating for distortions, using FNIRT tool in FSL. The T2-weighted TSE image was in turn rigidly registered to the 3D T1-weighted image, after skull stripping, and the latter was nonlinearly registered [Jenkinson and Smith, 2001] to MNI space. All previous transformations were concatenated and the inverse of the transformation was also calculated.

Six cortical regions (frontal cortex, motor cortex, postcentral cortex, posterior parietal cortex, temporal cortex, and occipital cortex) were derived using the Harvard-Oxford cortical atlas [Broser et al., 2011], as previously described [Behrens et al., 2003a].

Using SPM8 software, 3D T1 weighted images in MNI space were segmented into three classes (GM, WM, and CSF) and, after thresholding at 50%, binary masks were obtained.

The thalami were segmented from the 3D T1-weighted images in native space using the FIRST tool from the FMRIB Software Library [Patenaude et al., 2011]. This method uses shape and appearance models derived from a training set and defined in MNI space. To bring the models into native image space, normalization is performed using a two-stage linear registration, to achieve robust subcortical alignment. To improve the segmentation, in particular for the delimitation of the boundary with the internal capsule, the script was modified to calculate both stages of the linear registration, using single subject FA map and the FA template of FSL as reference. The results of segmentation were all visually checked. Normalized thalamic volumes were calculated from the FIRST output using the SIENAx scaling factor [Smith et al., 2002].

Thalamus and T2/T1 lesion masks were registered to MNI space using the previously calculated nonlinear registration.

Derivation of thalamic connectivity defined regions (CDR) and cortico-thalamic tracts

To avoid the effect of lesions on diffusion tractography, data from HCs were used to create CDR and cortico-thalamic tract probability maps to be applied to all study subjects [Pagani et al., 2005]. HC from the center with 12 DW directions were not used to create these probability maps. The probtrackx tool from FSL [Behrens et al., 2007] was used to perform probabilistic tractography with voxels in the thalamus used as seeds to draw 5,000 samples from the connectivity distribution and the six cortical regions as classification targets (curvature threshold = 0.2). This resulted in six thalamic maps, representing for each voxel of the thalamus the probability of connection to each of the six cortical regions. As both seed and target regions were defined in MNI space, the nonlinear registration was provided as input to the program. Finally, hard segmentation of the thalamus was performed classifying seed voxels based on the highest connection probability to target masks [Behrens et al., 2007; Johansen-Berg et al., 2005]. This approach has already been proven to be highly reproducible [Traynor et al., 2010]. This produced exclusive CDRs, which were averaged across HCs [Johansen-Berg et al., 2005] to obtain probability maps of each CDR: frontal CDR (F-CDR), motor CDR (M-CDR), postcentral CDR (PC-CDR), posterior parietal CDR (PP-CDR), temporal CDR (T-CDR), and occipital CDR (O-CDR) (Fig. 1) [Johansen-Berg et al., 2005].

Probability maps of WM tracts connecting each CDR to the corresponding cortical target were also obtained, using CDRs as seed regions and relative cortical masks as waypoints. The following tracts were obtained from each control: Fronto-Thalamic (F-T) tract, Motor-Thalamic (M-T) tract, Post-Central-Thalamic (PC-T) tract, Posterior-Parietal (PP-T) tract, Temporal-Thalamic (T-T) tract, and Occipital-Thalamic (O-T) tract. After exclusion of thalamic voxels, the previous tracts were normalized by the total number of generated tracts that were not rejected by inclusion/exclusion mask criteria, thresholded, binarized, and averaged to obtain tract probability maps in MNI space (Fig. 2).

Calculation of cortico-thalamic DT MRI, LV and atrophy measures

CDR and tract probability maps were transformed back to native space, thresholded at 33%, binarized and applied to DT MRI maps of all study subjects to obtain average values, after exclusion of lesions, CSF and overlapping voxels [Pagani et al., 2005]. In the same way, CDR and tract masks were applied to T2/T1 lesion masks transformed to the DTI space to calculate LV. The same

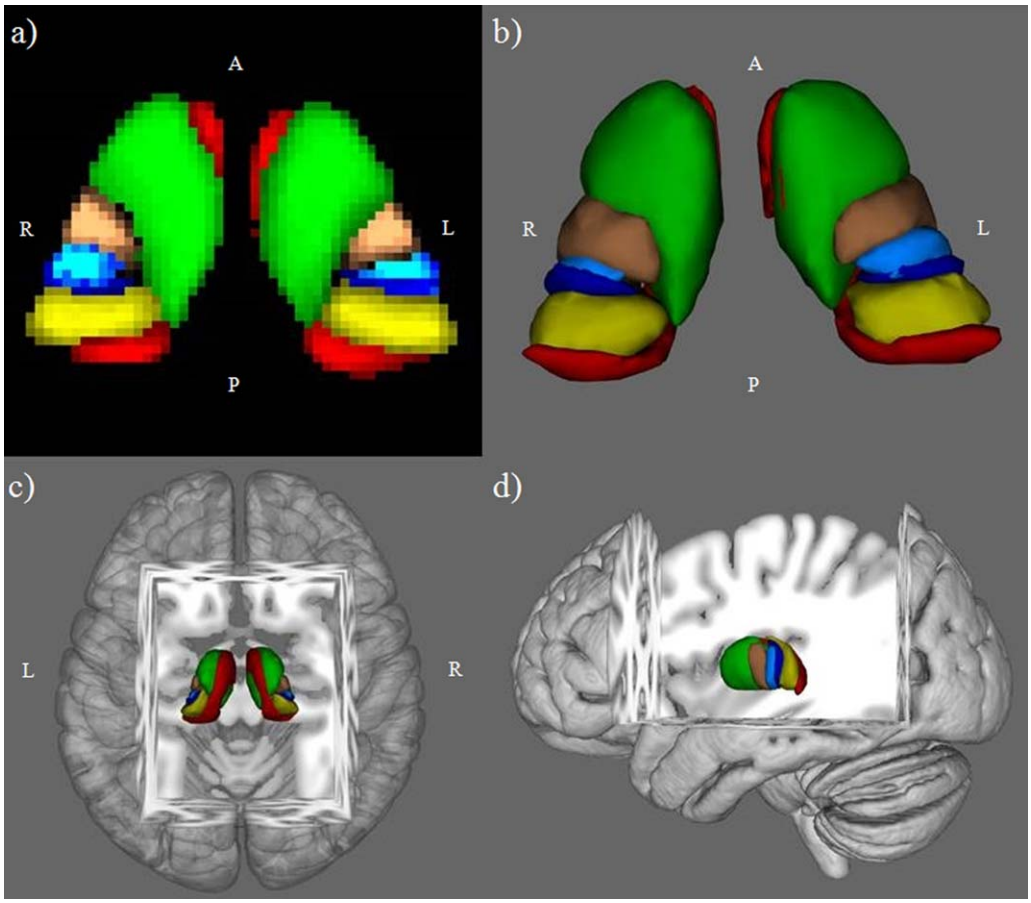

Figure 1.
Thalamic connectivity defined regions (CDRs) probability maps from healthy controls, thresholded at 33%, in Montreal Neurological Institute space: (a) axial 2D view; (b) ventral 3D view; (c) dorsal 3D view; and (d) left lateral 3D view. Green=frontal CDR, copper=motor CDR, light blue=postcentral CDR, blue=posterior parietal CDR, red=temporal CDR, yellow=occipital CDR. L, left; R, right; A, anterior; P, posterior.

procedure was used to calculate mean DT MRI indices and T2/T1 LV of the whole thalamus, bilaterally. The volume of each cortical target was calculated by applying cortical masks to single subject GM maps, after transforming them back to native space. These volumes were normalized using the SIENAx scaling factor [Smith et al., 2002].

Vertex analysis

To assess group differences of thalamic shape on a per-vertex basis, vertex analysis was performed using the signed, perpendicular distance from the average surface, calculated at each corresponding anatomical point by FIRST. The projections are scalar values, allowing them to be processed by univariate statistical methods (randomize tool, FSL 5.0.5). FIRST creates a surface mesh for each subcortical structure using a deformable mesh model. The mesh is composed of a set of triangles and the apex of adjoining triangles is called a vertex. The number of vertices for each structure is fixed so that corresponding vertices can be compared across individuals and between groups. Vertex correspondence is crucial for the FIRST method, as it facilitates the investigation of localized shape differences through the examination of group differences in the spatial location of each vertex. When reconstructed in MNI space, the surfaces have a common reference frame, although local pose differences may still exist. In addition to the global affine transformation, pose (rotation and translation) can be removed with a rigid transformation by minimizing the sum-of-squares difference between the corresponding vertices of a subject's surface and the mean surface (target). The following options were chosen: (a) "useReconMNI": to reconstruct the meshes in MNI

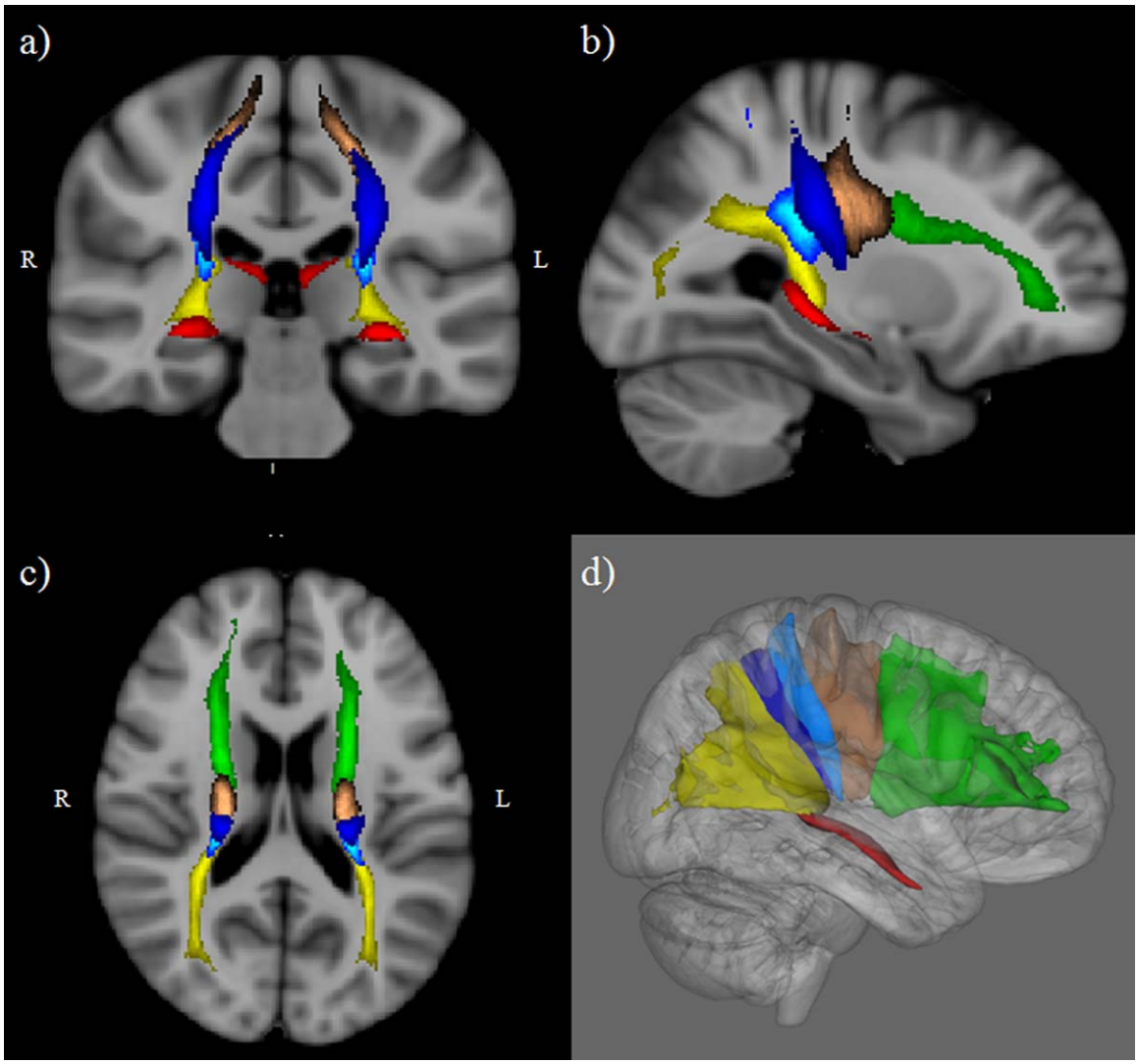

Figure 2.

Cortico-thalamic tracts probability maps from healthy controls, thresholded at 33%, in Montreal Neurological Institute space: (a) coronal 2D view; (b) sagittal 2D view; (c) axial 2D view; and (d) lateral 3D view of right tracts. Green=fronto-thalamic tract, copper=motor-thalamic tract, light blue=postcentral-thalamic tract, blue=posterior parietal-thalamic tract, red=temporo-thalamic tract, yellow=occipito-thalamic tract. L, left; R, right.

space; (b) "useRigidAlign": to remove additional differences between the meshes using a rigid transformation [Patenaude et al., 2011].

Summary of the Analysis

To summarize, the method consists of a first part aimed at relating native DTI space to MNI space. This is needed both for the construction of probability maps from HCs and for their application to patient data. In the second step, the thalami and cortical lobes are obtained. In the third one, tractography is applied to HC data to segment the thalami according to their cortical projections. CDR probability maps are also obtained. Finally, CDRs maps are applied to HC and patients data. The same procedure is used to study the tracts connecting each CDR region to the cortical lobes.

The following describes the four steps:

1. b0 to MNI: (a) brain extraction of the T2-weighted TSE image (native space); (b) rigid registration of the T2-weighted TSE image to the b0 EPI image; (c) non-linear deformation of the b0 image to match the

registered T2-weighted TSE (to compensate distortions); (d) linear registration of the T2-weighted TSE image to the 3D T1-weighted image; (e) nonlinear deformation of the 3D T1-weighted image to MNI space. All intermediate transformations are concatenated to relate native DTI space to MNI space. The inverse transformation is also calculated.
2. Thalamus and lobes segmentation: (a) segmentation of left and right thalamus using FIRST on the 3D T1-weighted image in native space; (b) thalamic masks are transformed to MNI space; (c) cortical lobes (in MNI space) are derived from the Harvard-Oxford cortical atlas.
3. Segmentation of the thalami in CDRs: (a) tractography is run using as input the DW data in native space, thalamus and cortical lobes masks in MNI space, the direct and inverse nonlinear transformation obtained at point 1. This results in six maps of probability that the thalamic voxels are connected to each lobe, saved in MNI space; (b) after hard segmentation of the results and average across subjects, CDR probability maps are produced.
4. Application to patient data: (a) CDR probability maps are transformed back to native space using the inverted nonlinear transformation calculated at point 1, thresholded and binarized; (b) relevant indices are obtained within each region.

Statistical Analysis

Between-group comparisons were performed using the Mann-Whitney test, Kruskal-Wallis test, and Chi-square test, as appropriate. Normal distribution assumption was checked by means of Q–Q plot and Shapiro-Wilk and Kolmogorov–Smirnov tests. Skewed distributed variables were log-transformed before analyses. MRI measures were compared between groups using a linear mixed model accounting for between-center heterogeneity, adjusting for subjects' age and sex. Pairwise *post hoc* comparisons were corrected for multiple comparisons using the Hochberg method. Multivariate linear mixed models were built assuming thalamic DT MRI variables as dependent variable and the following hypothetic determinants of thalamic damage as covariates: (1) for whole thalamus: side specific thalamic volume (right/left), side specific thalamic T2/T1 LV, NBV, NGMV, NWMV; (2) for each CDR: CDR T2/T1 LV, CDR related tract T2/T1 LV and DT MRI indices, specific cortical target volume. Thalamic covariates were selected using a stepwise variable selection method, with a significance level of 0.05 for them both to enter and to remain in the model.

A random forest analysis (RF) was run to identify the best predictors, among all MRI variables explored, of global cognitive impairment as well as impairment at specific cognitive domains [Breiman, 2001]. An output of the RF corresponds to variable importance reported as a ranking: each covariate receives a score according to its ability to classify correctly the patient's outcome when data are permuted. For easier interpretation, variable importance was normalized with respect to the best predictor. For RF analysis, MRI measures which showed significant correlation ($P<0.1$ using the Spearman Rank Correlation coefficient) with neuropsychological scores were considered (to overcome the problem of false positive discoveries, while preserving a small risk of false negative results).

All analyses were performed using SAS Release 9.3. For the RF analysis, we used the package "randomForest" version 4.5 implemented in the R software package.

RESULTS

Clinical, Neuropsychological, and Conventional MRI Measures

Table II summarizes the main conventional MRI features of MS patients as a whole and according to the presence/absence of cognitive impairment. Compared to HCs, MS patients had lower NBV ($P<0.0001$), NGMV ($P=0.001$) and NWMV ($P<0.0001$). A significant site effect was found for sex, age, EDSS, NBV, NGMV and NWMV, whereas no effect was found for disease duration, T2 LV and T1 LV (Table I).

Twenty-two (42%) MS patients were classified as CI. The domains most frequently involved were: attention and information processing speed (33% of the patients), executive functions (27%), verbal memory (21%), spatial memory (19%), and verbal fluency (19%) (Table III).

The distribution of CI and cognitively preserved (CP) patients did not differ significantly among sites (Table I). Compared to CP patients, CI MS patients were significantly older (mean age=37.9 years, SD=7.8 years for CP and 43.4 years, SD=8.6 years for CI patients; $P=0.03$), had higher EDSS (median EDSS=1.5, range 0–4.0 for CP and 2.0, range 1.0–6.0 for CI patients, $P=0.03$) and T1 LV ($P=0.04$), as well as lower NBV ($P=0.006$), NGMV ($P=0.009$) and NWMV($P=0.04$). No differences were found for sex ($P=0.10$), disease duration ($P=0.15$) and T2LV ($P=0.06$).

SNR

The SNR was greater than 20 for all sites (site 1=28, site 2=24, site 3 [with 12 DW directions]=49, Site 4=36, site 5=49, site 6= 42). According to the simulation published by Behrens et al. [2007], this allows two crossing fibers up to a separation angle of 60 degrees to be correctly modeled (for 30 DW directions and $b=1{,}000$).

Cortical Target Volumes

Table II summarizes cortical target volume measurements from HC and MS patients as a whole and according to the presence/absence of cognitive impairment. All cortical

TABLE II. Conventional MRI measures and CT normalized volumes in HC and MS patients with (CI) and without cognitive impairment (CP)

	HC (57)	MS (52)	P^a	CP MS patients (30)	CI MS patients (22)	P^a
Mean T2 LV (ml) (SD)	—	11.0 (13.9)	—	6.6 (7.3)	16.9 (18.2)	0.06
Mean T1 LV (ml) (SD)	—	5.7 (6.1)	—	3.4 (3.1)	8.9 (7.8)	0.04
Mean NBV (ml) (SD)	1526 (80)	1428 (113)	<0.0001	1455 (106)	1391 (114)	0.006
Mean NGMV (ml) (SD)	823 (56)	777 (70)	0.001	798 (70)	748 (59)	0.009
Mean NWMV (ml) (SD)	703 (41)	651 (71)	<0.0001	657 (54)	642 (89)	0.04
Mean F CT nVol (ml) (SD)	186.1 (19.1)	173.3 (22.2)	0.008	179.3 (21.8)	165.2 (20.4)	0.008
Mean M CT nVol (ml) (SD)	38.9 (4.3)	36.2 (5.9)	0.006	37.9 (5.5)	33.9 (5.8)	0.008
Mean PC CT nVol (ml) (SD)	24.7 (3.1)	23.1 (3.7)	0.006	24.3 (3.6)	21.3 (3.3)	0.002
Mean PP CT nVol (ml) (SD)	57.7 (6.3)	52.4 (7.1)	0.0002	54.0 (7.4)	50.2 (6.1)	0.05
Mean T CT nVol (ml) (SD)	136.0 (12.2)	122.8 (14.4)	<0.0001	127.0 (12.8)	117.1 (14.8)	0.005
Mean O CT nVol (ml) (SD)	147.1 (13.1)	135.1 (17.5)	0.0001	140.1 (16.3)	128.2 (17.1)	0.004

[a]Linear mixed model accounting for between-centre heterogeneity, adjusting for age; Hochberg method correction.
SD, standard deviation; HC, healthy controls; MS, multiple sclerosis; CP, cognitively preserved; CI, cognitively impaired; LV, lesion volume, CT, cortical target; nVol, normalized volume; F, frontal; M, motor; PC, postcentral; PP, posterior parietal; T, temporal; O, occipital.

targets volumes were significantly lower in MS patients versus HCs, in CI MS patients versus HCs and in CI versus CP MS patients. Compared to HCs, CP MS patients had lower PP-target (P=0.05) and T-target (P=0.008) volumes.

Whole and Regional Thalamic Damage

In line with previous MRI and histological findings [Broser et al., 2011; Harris et al., 1996; Watkins et al., 2001], DT MRI parameters of the left and right thalamus differed significantly both in HC and MS patients. For this reason, the left and right thalami were analyzed separately. Due to its variability in position, small size and frequent overlap with other areas in HCs, PP-CDR survived, after threshold and exclusion of overlapping voxels, only in a small number of patients. As a consequence, its derived measures were not considered in the statistical analysis.

The results of the between-group comparisons of whole and regional thalamic volumes and DT MRI measures are summarized in Table IV. Compared to HCs, MS patients had: (1) decreased thalamic volume, bilaterally; (2) increased FA in the thalamus, F-CDR and O-CDR, bilaterally; (3) increased MD in the bilateral F-CDR, bilateral T-CDR and bilateral O-CDR. Compared to HCs, CP MS patients had: (1) decreased bilateral thalamic volumes; (2) increased MD in the bilateral T-CDR. Compared to HCs, CI MS patients had: (1) decreased thalamic volume, bilaterally; (2) increased FA in the bilateral thalamus, bilateral F-CDR, left PC-CDR and bilateral O-CDR; (3) increased MD in the bilateral thalamus, bilateral F-CDR, left PC-CDR, bilateral T-CDR and bilateral O-CDR. Compared to CP, CI MS patients had: (1) decreased bilateral thalamic volumes; (2) increased FA in the bilateral F-CDR, M-CDR, PC-CDR and O-CDR; (3) increased MD in the left thalamus, bilateral F-CDR, right M-CDR, left PC-CDR, bilateral T-CDR, and bilateral O-CDR.

Global and regional thalamic T2 and T1 LV did not differ between CI and CP MS patients.

TABLE III. Number and frequency of patients with MS with abnormal performance at neuropsychological tests and distribution across centers

Cognitive domains	All centers (N=52)	Amsterdam (N=8)	Graz (N=6)	London (N=7)	Milan (N=10)	Naples (N=11)	Siena (N=10)
Attention/information processing speed (%)	17 (33%)	2 (25%)	2 (33%)	2 (29%)	6 (60%)	4 (36%)	1 (10%)
Executive functions (%)	14 (27%)	3 (38%)	1 (17%)	5 (71%)	4 (40%)	0 (0%)	1 (10%)
Verbal memory (%)	11 (21%)	3 (38%)	1 (17%)	2 (29 %)	2 (20%)	3 (27%)	0 (0%)
Spatial memory (%)	10 (19%)	0 (0%)	1 (17%)	2 (29%)	3 (30%)	3 (27%)	1 (10%)
Verbal fluency (%)	10 (19%)	2 (25%)	3 (50%)	0 (0%)	1 (10%)	4 (36%)	0 (0%)

Abnormalities of attention, verbal memory, spatial memory and verbal fluency domains were derived from the scores obtained at the Brief Repeatable Battery-Neuropsychological (BRB-N) battery, abnormalities of the executive functions were derived from the scores obtained at the WCST. See text for further details.

TABLE IV. Whole and regional thalamic damage in HC and MS patients with (CI) and without cognitive impairment (CP)

		LEFT THALAMUS					RIGHT THALAMUS				
Variable		HC	MS patients	P^a	CP MS patients	CI MS patients	P^a	HC	MS patients	P^a	CP MS patients	CI MS patients	P^a
nVol (ml]) (SD)		6.5 (0.8)	5.3 (1.1)	<0.0001	5.7 (0.8)	4.6 (1.0)	<0.0001	6.5 (0.8)	5.3 (1.0)	<0.0001	5.8 (0.8)	4.6 (0.9)	<0.0001
Whole (SD)	FA	0.34 (0.03)	0.35 (0.04)	0.04	0.34 (0.03)	0.36 (0.04)	n.s	0.33 (0.03)	0.34 (0.04)	0.03	0.34 (0.03)	0.35 (0.04)	n.s.
	MD	0.75 (0.04)	0.75 (0.05)	n.s.	0.74 (0.04)	0.76 (0.05)	0.004	0.75 (0.03)	0.75 (0.05)	n.s.	0.74 (0.03)	0.76 (0.06)	n.s.
F-CDR (SD)	FA	0.33 (0.03)	0.35 (0.05)	0.01	0.34 (0.04)	0.37 (0.06)	0.02	0.33 (0.03)	0.34 (0.05)	0.03	0.33 (0.03)	0.36 (0.06)	0.01
	MD	0.75 (0.03)	0.77 (0.07)	0.04	0.75 (0.04)	0.79 (0.09)	0.0009	0.76 (0.03)	0.78 (0.07)	0.0003	0.76 (0.04)	0.81 (0.09)	0.0003
M-CDR (SD)	FA	0.37 (0.06)	0.37 (0.08)	n.s.	0.35 (0.06)	0.41 (0.09)	0.01	0.37 (0.06)	0.37 (0.09)	n.s.	0.35 (0.06)	0.40 (0.11)	0.02
	MD	0.71 (0.04)	0.72 (0.06)	n.s.	0.71 (0.05)	0.72 (0.07)	n.s.	0.72 (0.03)	0.72 (0.05)	n.s.	0.71 (0.04)	0.74 (0.05)	0.006
PC-CDR (SD)	FA	0.39 (0.06)	0.40 (0.08)	n.s.	0.38 (0.07)	0.44 (0.09)	0.005	0.38 (0.07)	0.37 (0.07)	n.s.	0.35 (0.06)	0.40 (0.08)	0.02
	MD	0.72 (0.04)	0.72 (0.06)	n.s.	0.71 (0.04)	0.75 (0.07)	0.002	0.74 (0.04)	0.74 (0.06)	n.s.	0.74 (0.04)	0.75 (0.06)	n.s.
T-CDR (SD)	FA	0.34 (0.04)	0.33 (0.05)	n.s.	0.34 (0.05)	0.32 (0.05)	n.s.	0.35 (0.04)	0.33 (0.05)	n.s.	0.34 (0.04)	0.33 (0.06)	n.s.
	MD	0.81 (0.09)	1.01 (0.29)	<0.0001	0.90 (0.16)	1.16 (0.36)	<0.0001	0.81 (0.09)	1.00 (0.25)	<0.0001	0.92 (0.14)	1.12 (0.31)	0.0005
O-CDR (SD)	FA	0.33 (0.04)	0.35 (0.05)	0.0005	0.34 (0.03)	0.38 (0.07)	0.005	0.33 (0.05)	0.35 (0.06)	0.0009	0.34 (0.05)	0.37 (0.07)	0.007
	MD	0.77 (0.04)	0.80 (0.10)	0.01	0.77 (0.07)	0.84 (0.12)	0.003	0.77 (0.04)	0.82 (0.14)	0.002	0.78 (0.09)	0.87 (0.17)	0.002

[a]Linear mixed model accounting for between-centre heterogeneity, adjusting for age and sex; Hochberg method correction.
SD, standard deviation; HC, healthy controls; MS, multiple sclerosis; CP, cognitively preserved; CI, cognitively impaired; nVol, normalized volume; CDR, connectivity defined region; F, frontal; M, motor; PC, postcentral; T, temporal; O, occipital.
Average is expressed in units in $mm^2/s*10$ e -3, FA is a dimensionless index.

Cortico-Thalamic Tracts

The results of the between-group comparisons of DT MRI measures of the normal-appearing white matter (NAWM) and T2/T1 LV of each cortico-thalamic tract are summarized in Table V. Compared to HCs, MS patients had: (1) decreased FA in the bilateral T-T tract and bilateral O-T tract; and (2) increased MD in all tracts, except for bilateral PC-T tract. Compared to HCs, CP MS patients showed: (1) decreased FA in the T-T tract and O-T tract, bilaterally and (2) increased MD in all tracts, except for bilateral PC-T tract. Compared to HCs, CI MS patients showed: (1) decreased FA in the left PP-T tract, bilateral T-T tract and bilateral O-T tract and (2) increased MD in all tracts, except for right PC-T tract. Compared to CP, CI MS patients had: (1) decreased FA in the bilateral T-T tract and bilateral O-T tract and (2) increased MD in the bilateral F-T tract, bilateral M-T tract, left PC-T tract, left PP-T tract, bilateral T-T tract, and bilateral O-T tract.

Compared to CP patients, CI MS patients had higher T2 LV of the bilateral F-T tract and left O-T tract (P values ranging between 0.002 and 0.02) and higher T1 LV of the right F-T tract, left PP-T tract and right O-T tract (P values ranging from 0.001 to 0.04).

Thalamic Shape Analysis

Between-group comparisons of vertex analysis revealed significant atrophy ($P<0.05$) in: (1) MS patients versus HCs in the whole thalamus, bilaterally; (2) CP MS patients versus HCs in the whole thalamus, bilaterally, except for the left M-CDR, left PC-CDR and posterior-medial portion of T-CDR, bilaterally; (3) CI MS patients versus HCs in the whole thalamus, bilaterally; (4) CI versus CP MS patients in the whole right thalamus and in the left thalamus, except for the PP-CDR, O-CDR and posterior portion of T-CDR (Fig. 3). At a $P<0.01$, the distribution of atrophy in the right and left thalamus was similar.

Determinants of Thalamic Damage

Global thalamic FA was not associated with any parameters of the model. For all FA CDRs, except for right PC-CDR, the principal association was found with FA in the corresponding cortico-thalamic tract (P ranging from 0.0003 to <0.0001, partial R square=0.1–0.3, slope=0.4–0.9). For all MD CDRs, the principal association was found with MD in the corresponding cortico-thalamic tract ($P<0.0001$, partial R square=0.3–0.4, slope=0.8–1.3).

Random Forest Analysis

Figure 4 summarizes the results of RF analysis performed to identify the MRI variables significantly associated with global cognitive performance as well as with performance at specific cognitive domains. Whenever

TABLE V. Diffusion tensor MRI measures of cortico-thalamic tracts in HC and MS patients with (CI) and without cognitive impairment (CP)

		LEFT TRACTS						RIGHT TRACTS					
Variable		HC	MS patients	P^a	CP MS patients	CI MS patients	P^a	HC	MS patients	P^a	CP MS patients	CI MS patients	P^a
F-T tract (SD)	FA	0.47 (0.03)	0.46 (0.03)	n.s.	0.46 (0.03)	0.47 (0.03)	n.s	0.47 (0.03)	0.46 (0.03)	n.s.	0.45 (0.03)	0.46 (0.03)	n.s.
	MD	0.75 (0.04)	0.79 (0.06)	<0.0001	0.77 (0.05)	0.80 (0.07)	0.009	0.76 (0.03)	0.79 (0.06)	<0.0001	0.77 (0.04)	0.81 (0.07)	0.002
M-T tract (SD)	FA	0.50 (0.04)	0.49 (0.04)	n.s.	0.50 (0.03)	0.50 (0.05)	n.s.	0.50 (0.03)	0.49 (0.04)	n.s.	0.49 (0.03)	0.49 (0.04)	n.s.
	MD	0.71 (0.03)	0.73 (0.04)	<0.0001	0.72 (0.03)	0.75 (0.05)	0.01	0.72 (0.03)	0.74 (0.05)	<0.0001	0.73 (0.03)	0.76 (0.06)	0.02
PC-T tract (SD)	FA	0.48 (0.03)	0.47 (0.03)	n.s.	0.48 (0.03)	0.46 (0.03)	n.s.	0.48 (0.04)	0.47 (0.04)	n.s.	0.47 (0.03)	0.46 (0.04)	n.s.
	MD	0.74 (0.03)	0.74 (0.04)	n.s.	0.77 (0.05)	0.74 (0.03)	0.002	0.75 (0.04)	0.76 (0.05)	n.s.	0.74 (0.03)	0.77 (0.06)	n.s.
PP-T tract (SD)	FA	0.43 (0.04)	0.42 (0.03)	n.s.	0.43 (0.03)	0.41 (0.03)	n.s.	0.46 (0.05)	0.44 (0.06)	n.s.	0.45 (0.06)	0.43 (0.05)	n.s.
	MD	0.78 (0.04)	0.81 (0.06)	<0.0001	0.80 (0.05)	0.83 (0.07)	0.02	0.79 (0.05)	0.83 (0.07)	0.002	0.82 (0.07)	0.84 (0.06)	n.s.
T-T tract (SD)	FA	0.40 (0.03)	0.34 (0.05)	<0.0001	0.35 (0.03)	0.32 (0.05)	0.007	0.40 (0.03)	0.33 (0.04)	<0.0001	0.34 (0.04)	0.32 (0.04)	0.01
	MD	1.03 (0.10)	1.25 (0.23)	<0.0001	1.18 (0.16)	1.34 (0.27)	0.0003	1.03 (0.08)	1.26 (0.21)	<0.0001	1.17 (0.15)	1.37 (0.23)	<0.0001
O-T tract (SD)	FA	0.51 (0.04)	0.47 (0.04)	<0.0001	0.48 (0.04)	0.46 (0.04)	0.008	0.51 (0.03)	0.47 (0.04)	<0.0001	0.48 (0.04)	0.45 (0.04)	0.001
	MD	0.80 (0.07)	0.85 (0.06)	<0.0001	0.82 (0.05)	0.88 (0.06)	0.009	0.80 (0.04)	0.87 (0.07)	<0.0001	0.84 (0.05)	0.90 (0.08)	0.0009

[a]Linear mixed model accounting for between-centre heterogeneity, adjusting for age and sex; Hochberg method correction.
SD, standard deviation; HC, healthy controls; MS, multiple sclerosis; CP, cognitively preserved; CI, cognitively impaired; F-T, fronto-thalamic; M-T, motor-thalamic; PC-T, postcentral-thalamic; PP-T, posterior parieto-thalamic; T-T, tempo-thalamic; O-T, occipito-thalamic; FA, fractional anisotropy; MD, mean diffusivity.
Average MD is expressed in units in $mm^2/s*10\ e-3$, FA is a dimensionless index.

possible, the five most important MRI predictors are listed. The best predictor of global cognitive performance was left O-T tract MD. Considering performance at specific cognitive domains, impairment of attention/information processing speed was predicted by T1 LV of the left O-T Tract, followed by T2 LV of the left F-T tract; verbal memory impairment was predicted by MD in the left F-CDR, followed by MD in the right F-CDR; spatial memory impairment was associated with T1 LV of left M-T tract followed by MD in the left T-T tract; verbal fluency impairment was associated with FA in the O-CDR and MD in the left F-T tract; finally executive function was associated with MD in the right F-CDR and T2 LV of the right PC-T tract.

DISCUSSION

In this cross-sectional multicenter study, we applied advanced MRI techniques and sophisticated methods of analysis to investigate cortico-thalamic disconnection and its contribution to cognitive dysfunction in RRMS patients. To this aim, we used a validated and reproducible method to segment the thalamus in six CDRs, based on their cortical connections [Behrens et al., 2003a; Johansen-Berg et al., 2005; Traynor et al., 2010].

Our analysis of global thalamic atrophy provided results which are in line with the available literature in MS, that is that thalamic atrophy occurs in RRMS patients [Minagar et al., 2013] and is more severe in patients with cognitive impairment [Batista et al., 2012; Benedict et al., 2006, 2004; Houtchens et al., 2007].

The core results of our study are those obtained by the analysis of regional DT MRI parameters derived from thalamic normal appearing (NA) tissues (with the exclusion of focal visible lesions), which showed significant modifications in MS patients compared to HCs. We will discuss, in particular, FA abnormalities detected in this structure rather than MD ones, since they have been largely debated in literature and harbour major speculative implications [Cappellani et al. 2014b; Ciccarelli et al., 2001; Hannoun et al., 2012; Mesaros et al., 2011; Tovar-Moll et al., 2009]. Compared to HCs, MS patients experienced significantly increased FA in the whole thalamus, F-CDR and O-CDR, bilaterally, with a similar trend in all regions, except for bilateral T-CDRs, where a trend toward a reduced FA was found. Increased MD in the bilateral F-CDRs, T-CDRs and O-CDRs was also present. An increased FA in the thalamus in MS patients has already been described by several studies [Ciccarelli et al., 2001; Hannoun et al., 2012; Tovar-Moll et al., 2009], using different methodologies. Specifically, previous thalamic DT MRI studies applied either a region-of-interests analysis, without considering the anatomical connections and subdivisions of this structure, or sampled the thalamus as a whole. Importantly, decreased thalamic FA in patients with MS [Cappellani et al., 2014b; Mesaros et al., 2011] and clinically isolated syndromes

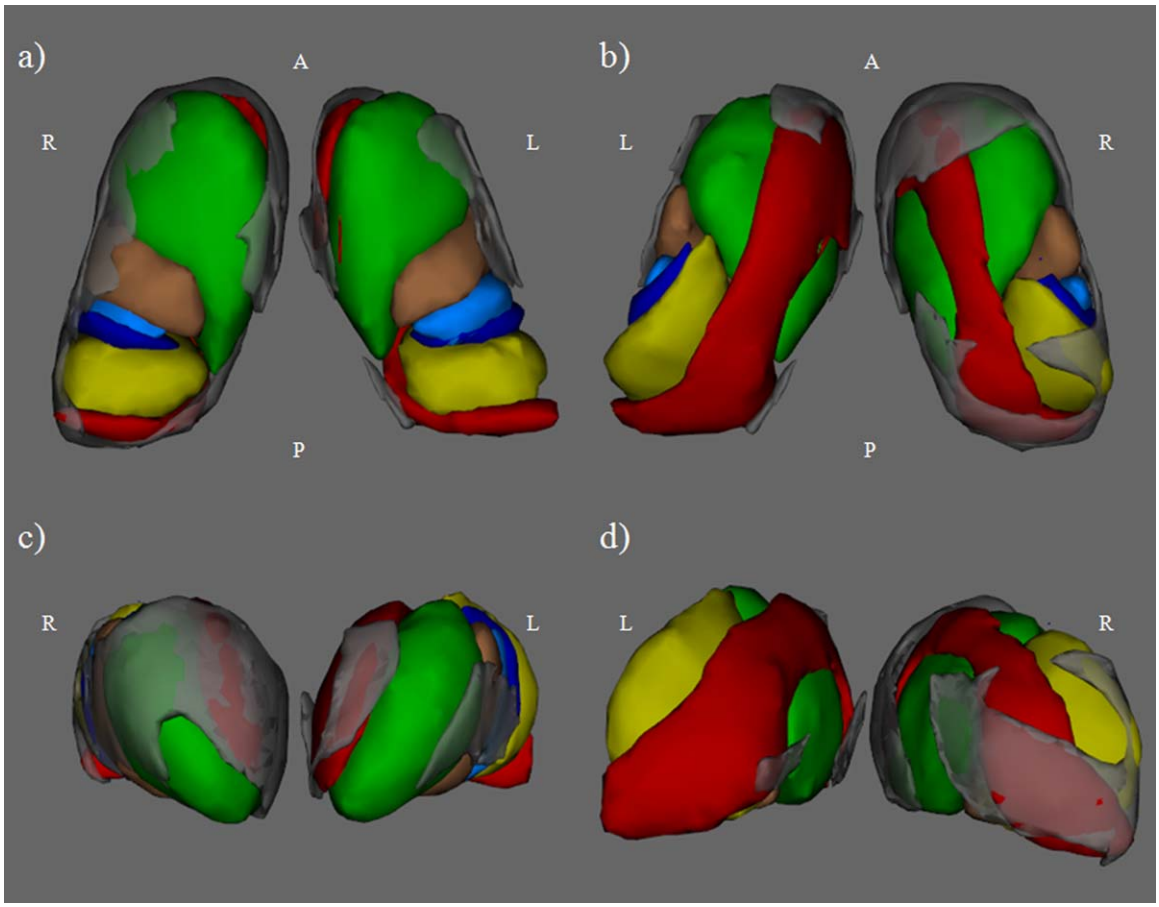

Figure 3.

Results of vertex analysis in CI versus CP multiple sclerosis (MS) patients for the left and right thalami overlaid on thalamic connectivity defined regions (CDRs) in Montreal Neurological Institute space: (a) ventral 3D view; (b) dorsal 3D view; (c) anterior 3D view; and (d) posterior 3D view. Gray represents the region of the thalamus more atrophic in CI versus CP MS patients ($P<0.05$). Green=frontal CDR, copper=motor CDR, light blue=postcentral CDR, blue=posterior parietal CDR, red=temporal CDR, yellow=occipital CDR. L, left; R, right; A, anterior; P, posterior.

(CIS) [Cappellani et al. 2014a] has also been reported. Various factors might contribute to explain discrepancies among available studies, including not only clinical characteristics of patients studied, but also the technique applied to segment the thalamus. In this regard, one potential problem is the contrast at the boundaries with the internal capsule that smoothly degrades due to the presence of WM fibers terminating in the thalamus. We tried to control for this using the contrast offered by FA maps for improving the segmentation (see methods). Other approaches might have biased their results by the contamination of WM surrounding the thalamus.

Regional and side differences of FA behavior can be explained by the complex structure of the thalamus and the previously described left/right thalamic asymmetries [Harris et al., 1996; Watkins et al., 2001]. The thalamus is composed of GM nuclear groups interconnected by highly anisotropic WM fascicles [Hannoun et al., 2012]. Additionally, thalamic GM also appears to show some degree of anisotropy that might be explained by the origin or termination of myelinated tracts. The increased FA detected in the majority of thalamic regions, although not always significant, may be an expression of a more prominent GM damage (or a greater effect of damaged GM due to its proportion in interested areas). Notably, increased FA has also been detected in cortical GM of MS patients [Calabrese et al., 2011; Filippi et al., in press; Poonawalla et al., 2008] and has been related to alterations of the neuronal cell micro-organization, including loss of dendritic arborization [Mukherjee et al., 2002], synaptic stripping [Hasbani et al., 2001] and local activation of microglia cells [Hannoun et al., 2012]. In contrast to the other thalamic regions, the T-CDR showed a nonsignificant reduction of FA in MS patients, which might reflect the presence of intrathalamic

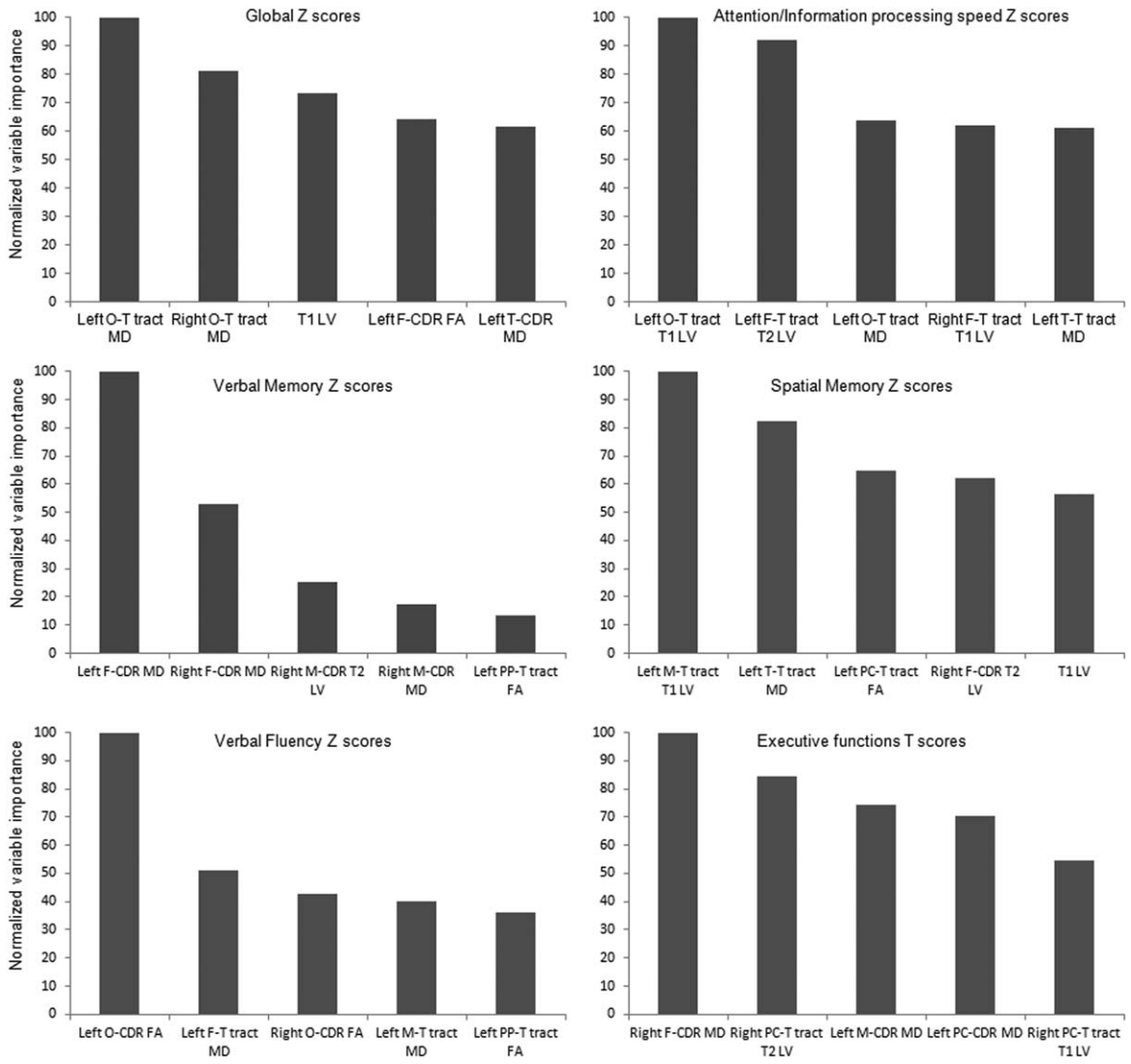

Figure 4.

Results of the random forest analysis. Normalized variable importance of the five most important MRI variables in predicting global and specific cognitive scores. For verbal memory, only four variables were associated. MD, mean diffusivity; FA, fractional anisotropy; LV, lesion volume; CDR, connectivity defined region; Thal, thalamic; F, frontal; M, motor; PC, postcentral; F-T, fronto-thalamic; M-T, motor-thalamic; PC-T, postcentral-thalamic; PP-T, posterior parietal-thalamic; O-T, occipito-thalamic.

WM damage in thalamic subregions with a higher proportion of WM [Hannoun et al., 2012]. As a consequence, FA decrease in intrathalamic WM and in thalamic origin/termination of myelinated tracts could balance the increase of intrathalamic GM FA [Hannoun et al., 2012].

Compared to CP MS patients, those with CI had higher FA in the bilateral F-CDR, M-CDR, PC-CDR and O-CDR. The most prominent increase of FA observed in CI MS patients could be explained by a more severe damage to the GM in this group. F-CDR involves parts of the anterior nuclear complex, which has an essential role in cognition because of its projection to prefrontal areas [Behrens et al. 2003a]. M-CDR includes voxels connecting to motor and premotor areas and contains the ventral anterior nucleus, ventro-lateral anterior, and posterior nuclei [Behrens et al., 2003a], which are relevant for integration between subcortical structures and motor and premotor cortical areas [Nieuwenhuys et al., 2008]. In addition, regional analysis of thalamic atrophy showed greater involvement of anterior regions (including F-CDR and M-CDR) in CI MS patients. In support of this, a previous study in HCs has shown more severe atrophy with aging in the anterior portion of the thalamus, involving regions containing the anterior and dorso-medial nuclei [Hughes et al., 2012].

The O-CDR contains some intralaminar nuclei [Behrens et al., 2003a], which are relevant in integration of functions, receiving converging inputs from many different structures, projecting diffusely to the cortex and being interconnected extensively with the reticular thalamic nucleus [Nieuwenhuys et al., 2008]. As a consequence, their involvement could be expression of the relevance of integrating function of thalamic nuclei for cognition. To summarize, we postulate that increased FA observed in the majority of thalamic subregions might reflect prominent GM damage, more relevant in CI MS patients. The decreased FA observed in T-CDR, although not significant, is likely related to WM damage, present in all MS patients.

Our approach also enabled us to estimate DT MRI indices in the WM tracts connecting the different thalamic subregions to the cortex. In agreement with several DT MRI studies, such an analysis showed decreased FA and increased MD in the majority of the tracts analyzed [Dineen et al., 2009; Hulst et al., 2013; Mesaros et al., 2012; Yu et al., 2012). While MD abnormalities affected diffusely these WM tracts, FA decrease was restricted to a few tracts, and in particular to the bilateral T-T tract and bilateral O-T tract in the comparison between CI and CP MS patients. Surprisingly, FA reduction was not found in the F-T tract, which is particularly relevant for cognition [Hughes et al., 2012]. Such a negative result might be due to the wide extension of the F-T tract, which involves also areas where WM tracts are less coherently oriented, with a consequent reduction of FA sensitivity to detect significant abnormalities [Jones, 2003].

To define if and how damage in a given pathway influenced regional thalamic abnormalities, we also investigated the association between CDR damage and abnormalities of other components of the cortico-thalamic circuit, specific for each CDR. Interestingly, such an analysis demonstrated that for all FA CDRs (except for right PC-CDR), the principal association was with FA in the corresponding cortico-thalamic tract, with a positive slope. It is tempting to speculate that these findings could reflect an influence of NAWM tract damage on the CDR abnormalities possibly due to demyelination and that thalamic GM damage might be a partially independent process.

To assess which of the many variables analyzed played a prominent role in explaining global and specific cognitive dysfunction, we used a RF approach, which allows robust estimation of the associations between different variables. The RF approach is an established and highly accurate classifier, which can handle a large number of input variables even when the number of observations is small. Unlike a classic correlation analysis, no adjustment for multiple comparisons is needed. By introducing an appropriate level of randomness, it produces accurate estimates of associations handling the problem of correlated predictors and showing which among them is the best one [Breiman, 2001]. Not unexpectedly, RF analysis demonstrated that damage to specific thalamo-cortical connections explained patients' global cognitive profile as well as impairment at specific cognitive tests, thus confirming the notion that cognitive impairment in MS is mostly the result of a cortico-subcortical disconnection [Dineen et al., 2009; Hulst et al., 2013; Mesaros et al., 2009, 2012]. In particular, O-T tract damage was the most relevant predictor of global cognitive dysfunction, followed by T1 LV and regional thalamic diffusivity abnormalities. Attention/information processing speed performance was substantially modulated by focal lesions in WM tracts connecting the thalamus with occipital and frontal areas, particularly relevant for this function [Chiaravalloti and DeLuca 2008; Whelan et al., 2010]. Verbal memory performance was associated with MD in the left F-CDR, confirming the relevant role of these thalamic areas in cognitive functions. Spatial memory deficits were associated with damage to M-T and T-T tracts, connecting thalamic subregions (with relevant integrations functions) with frontal ant temporal areas, implicated with this function [van Asselen et al., 2006; Whelan et al., 2010]. Disconnection between the thalamus and the cortex as a causative mechanism of cognitive deficits is also supported by the association between verbal fluency performance and damage to M-T tracts as well as between executive functions and damage to the M-CDR.

Our study is not without limitations. First, the small sample size and the variability of DT MRI in a multicenter context may limit the general applicability of our findings. To mitigate this issue, we used a DT MRI sequence and statistical approach previously tested in a multicenter setting [Pagani et al., 2010]. To increase the number of subjects in the study, we included a site with an acquisition scheme of 12 DW directions. Although not optimal for the study of the WM [Jones, 2004], such a scheme can be considered sufficient for limiting the variability of FA and MD in the thalamic GM [Jones, 2004]. Clearly, the low angular resolution sampling in this case did not allow estimation of the 2 fibers modeled per voxel. To mitigate this effect, data from this center were not used to build probability maps. Second, despite age being included as a covariate in all statistical analyses, we cannot completely rule out the possibility that our findings were influenced by the MS patients being older than the HCs. Third, we used HC derived masks to extract DT MRI values in MS patients, due to limitations of the tractography approach in the context of this pathology; the working hypothesis is that the shapes of CDRs are preserved in MS patients or that their modifications can be captured by a nonlinear warping from changes at the thalamic boundaries. Forth, using tractography-based segmentation we were unable to separate thalamic WM and GM to better characterize FA modifications within this structure. In the same way, the use of the tensor model and its derived indices does not allow separation of the contribution of different fiber tracts that cross within a voxel. More sophisticated approaches, such as a multitensor model, are needed for this purpose. Fifthly, the use of the same set of HCs both for creating the probability maps and for extracting HCs metrics may

have biased the results. Finally, in the study of the determinants of thalamic damage, we did not consider subcortical and spinal regions connected with the thalamus.

In conclusion, our study shows that cortico-thalamic disconnection is, at various levels, implicated in cognitive dysfunction in MS. These results, obtained in a multicenter context, encourage the use of thalamic measures in multicenter studies, such as clinical trials, of these patients.

REFERENCES

Basser PJ, Mattiello J, LeBihan D (1994): Estimation of the effective self-diffusion tensor from the NMR spin echo. J Magn Reson B 103:247–254.

Batista S, Zivadinov R, Hoogs M, Bergsland N, Heininen-Brown M, Dwyer MG, Weinstock-Guttman B, Benedict RH (2012): Basal ganglia, thalamus and neocortical atrophy predicting slowed cognitive processing in multiple sclerosis. J Neurol 259: 139–146.

Behrens TE, Johansen-Berg H, Woolrich MW, Smith SM, Wheeler-Kingshott CA, Boulby PA, Barker GJ, Sillery EL, Sheehan K, Ciccarelli O, Thompson AJ, Brady JM, Matthews PM (2003a): Non-invasive mapping of connections between human thalamus and cortex using diffusion imaging. Nat Neurosci 6:750–757.

Behrens TE, Woolrich MW, Jenkinson M, Johansen-Berg H, Nunes RG, Clare S, Matthews PM, Brady JM, Smith SM (2003b): Characterization and propagation of uncertainty in diffusion-weighted MR imaging. Magn Reson Med 50:1077–1088.

Behrens TE, Berg HJ, Jbabdi S, Rushworth MF, Woolrich MW (2007): Probabilistic diffusion tractography with multiple fibre orientations: What can we gain? Neuroimage 34:144–155.

Benedict RH, Weinstock-Guttman B, Fishman I, Sharma J, Tjoa CW, Bakshi R (2004): Prediction of neuropsychological impairment in multiple sclerosis: Comparison of conventional magnetic resonance imaging measures of atrophy and lesion burden. Arch Neurol 61:226–230.

Benedict RH, Bruce JM, Dwyer MG, Abdelrahman N, Hussein S, Weinstock-Guttman B, Garg N, Munschauer F, Zivadinov R (2006): Neocortical atrophy, third ventricular width, and cognitive dysfunction in multiple sclerosis. Arch Neurol 63:1301–1306.

Benedict RH, Hulst HE, Bergsland N, Schoonheim MM, Dwyer MG, Weinstock-Guttman B, Geurts JJ, Zivadinov R (2013): Clinical significance of atrophy and white matter mean diffusivity within the thalamus of multiple sclerosis patients. Mult Scler 19:1478–1484.

Boringa JB, Lazeron RH, Reuling IE, Ader HJ, Pfennings L, Lindeboom J, de Sonneville LM, Kalkers NF, Polman CH (2001): The brief repeatable battery of neuropsychological tests: Normative values allow application in multiple sclerosis clinical practice. Mult Scler 7:263–267.

Breiman L (2001): Random forests. Mach Learn 45:5–32.

Broser P, Vargha-Khadem F, Clark CA (2011): Robust subdivision of the thalamus in children based on probability distribution functions calculated from probabilistic tractography. Neuroimage 57:403–415.

Calabrese M, Rinaldi F, Seppi D, Favaretto A, Squarcina L, Mattisi I, Perini P, Bertoldo A, Gallo P (2011): Cortical diffusion-tensor imaging abnormalities in multiple sclerosis: A 3-year longitudinal study. Radiology 261:891–898.

Cappellani R, Bergsland N, Weinstock-Guttman B, Kennedy C, Carl E, Ramasamy DP, Hagemeier J, Dwyer MG, Patti F, Zivadinov R (2014a): Diffusion tensor MRI alterations of subcortical deep gray matter in clinically isolated syndrome. J Neurol Sci 338:128–134.

Cappellani R, Bergsland N, Weinstock-Guttman B, Kennedy C, Carl E, Ramasamy DP, Hagemeier J, Dwyer MG, Patti F, Zivadinov R (2014b): Subcortical deep gray matter pathology in patients with multiple sclerosis is associated with white matter lesion burden and atrophy but not with cortical atrophy: A diffusion tensor MRI study. AJNR Am J Neuroradiol 35:912–919.

Chard DT, Jackson JS, Miller DH, Wheeler-Kingshott CA (2010): Reducing the impact of white matter lesions on automated measures of brain gray and white matter volumes. J Magn Reson Imaging 32:223–228.

Chiaravalloti ND, DeLuca J (2008): Cognitive impairment in multiple sclerosis. Lancet Neurol 7:1139–1151.

Ciccarelli O, Werring DJ, Wheeler-Kingshott CA, Barker GJ, Parker GJ, Thompson AJ, Miller DH (2001): Investigation of MS normal-appearing brain using diffusion tensor MRI with clinical correlations. Neurology 56:926–933.

Dietrich O, Raya JG, Reeder SB, Reiser MF, Schoenberg SO (2007): Measurement of signal-to-noise ratios in MR images: Influence of multichannel coils, parallel imaging, and reconstruction filters. J Magn Reson Imaging 26:375–385.

Dineen RA, Vilisaar J, Hlinka J, Bradshaw CM, Morgan PS, Constantinescu CS, Auer DP (2009): Disconnection as a mechanism for cognitive dysfunction in multiple sclerosis. Brain 132: 239–249.

Filippi M, Riccitelli G, Mattioli F, Capra R, Stampatori C, Pagani E, Valsasina P, Copetti M, Falini A, Comi G, Rocca MA (2012): Multiple sclerosis: Effects of cognitive rehabilitation on structural and functional MR imaging measures—An explorative study. Radiology 262:932–940.

Filippi M, Preziosa P, Pagani E, Copetti M, Mesaros S, Colombo B, Horsfield M, Falini A, Comi G, Lassmann H, Rocca MA (2013): Microstructural MR imaging of cortical lesion in multiple sclerosis. Mult Scler 19:418–426.

Gronwall DM (1977): Paced auditory serial-addition task: A measure of recovery from concussion. Percept Mot Skills 44:367–373.

Hannoun S, Durand-Dubief F, Confavreux C, Ibarrola D, Streichenberger N, Cotton F, Guttmann CR, Sappey-Marinier D (2012): Diffusion tensor-MRI evidence for extra-axonal neuronal degeneration in caudate and thalamic nuclei of patients with multiple sclerosis. AJNR Am J Neuroradiol 33:1363–1368.

Harris JA, Guglielmotti V, Bentivoglio M (1996): Diencephalic asymmetries. Neurosci Biobehav Rev 20:637–643.

Hasbani MJ, Schlief ML, Fisher DA, Goldberg MP (2001): Dendritic spines lost during glutamate receptor activation reemerge at original sites of synaptic contact. J Neurosci 21:2393–2403.

Heaton RK, Chelune GJ, Talley JL, Kay GG, Curtis G (1993): Wisconsin Card sorting test (WCST) manual revised and expanded. Odessa, FL. Psychological Assessment Resources.

Henry RG, Shieh M, Okuda DT, Evangelista A, Gorno-Tempini ML, Pelletier D (2008): Regional grey matter atrophy in clinically isolated syndromes at presentation. J Neurol Neurosurg Psychiatry 79:1236–1244.

Houtchens MK, Benedict RH, Killiany R, Sharma J, Jaisani Z, Singh B, Weinstock-Guttman B, Guttmann CR, Bakshi R (2007): Thalamic atrophy and cognition in multiple sclerosis. Neurology 69:1213–1223.

Hughes EJ, Bond J, Svrckova P, Makropoulos A, Ball G, Sharp DJ, Edwards AD, Hajnal JV, Counsell SJ (2012): Regional changes in thalamic shape and volume with increasing age. Neuroimage 63:1134–1142.

Hulst HE, Steenwijk MD, Versteeg A, Pouwels PJ, Vrenken H, Uitdehaag BM, Polman CH, Geurts JJ, Barkhof F (2013): Cognitive impairment in MS: Impact of white matter integrity, gray matter volume, and lesions. Neurology 80:1025–1032.

Jenkinson M, Smith S (2001): A global optimisation method for robust affine registration of brain images. Med Image Anal 5: 143–156.

Johansen-Berg H, Behrens TE, Sillery E, Ciccarelli O, Thompson AJ, Smith SM, Matthews PM (2005): Functional-anatomical validation and individual variation of diffusion tractography-based segmentation of the human thalamus. Cereb Cortex 15: 31–39.

Johnson MD, Ojemann GA (2000): The role of the human thalamus in language and memory: Evidence from electrophysiological studies. Brain Cogn 42:218–230.

Jones DK (2003): Determining and visualizing uncertainty in estimates of fiber orientation from diffusion tensor MRI. Magn Reson Med 49:7–12.

Jones DK (2004): The effect of gradient sampling schemes on measures derived from diffusion tensor MRI: A Monte Carlo study. Magn Reson Med 51:807–815.

Lazeron RH, Boringa JB, Schouten M, Uitdehaag BM, Bergers E, Lindeboom J, Eikelenboom MI, Scheltens PH, Barkhof F, Polman CH (2005): Brain atrophy and lesion load as explaining parameters for cognitive impairment in multiple sclerosis. Mult Scler 11:524–531.

Lublin FD, Reingold SC (1996): Defining the clinical course of multiple sclerosis: Results of an international survey. National Multiple Sclerosis Society (USA) Advisory Committee on Clinical Trials of New Agents in Multiple Sclerosis. Neurology 46: 907–911.

Magon S, Chakravarty MM, Amann M, Weier K, Naegelin Y, Andelova M, Radue EW, Stippich C, Lerch JP, Kappos L, Sprenger T (2014): Label-fusion-segmentation and deformation-based shape analysis of deep gray matter in multiple sclerosis: The impact of thalamic subnuclei on disability. Hum Brain Mapp 35:4193–4203.

Mattioli F, Stampatori C, Zanotti D, Parrinello G, Capra R (2010): Efficacy and specificity of intensive cognitive rehabilitation of attention and executive functions in multiple sclerosis. J Neurol Sci 288:101–105.

Mesaros S, Rocca MA, Riccitelli G, Pagani E, Rovaris M, Caputo D, Ghezzi A, Capra R, Bertolotto A, Comi G, Filippi M (2009): Corpus callosum damage and cognitive dysfunction in benign MS. Hum Brain Mapp 30:2656–2666.

Mesaros S, Rocca MA, Pagani E, Sormani MP, Petrolini M, Comi G, Filippi M (2011): Thalamic damage predicts the evolution of primary-progressive multiple sclerosis at 5 years. AJNR Am J Neuroradiol 32:1016–1020.

Mesaros S, Rocca MA, Kacar K, Kostic J, Copetti M, Stosic-Opincal T, Preziosa P, Sala S, Riccitelli G, Horsfield MA, Drulovic J, Comi G, Filippi M (2012): Diffusion tensor MRI tractography and cognitive impairment in multiple sclerosis. Neurology 78:969–975.

Minagar A, Barnett MH, Benedict RH, Pelletier D, Pirko I, Sahraian MA, Frohman E, Zivadinov R (2013): The thalamus and multiple sclerosis: Modern views on pathologic, imaging, and clinical aspects. Neurology 80:210–219.

Mukherjee P, Miller JH, Shimony JS, Philip JV, Nehra D, Snyder AZ, Conturo TE, Neil JJ, McKinstry RC (2002): Diffusion-tensor MR imaging of gray and white matter development during normal human brain maturation. AJNR Am J Neuroradiol 23: 1445–1456.

Nieuwenhuys R, Voogd J, Huijzen CV (2008): The Human Central Nervous System. New York: Springer. xiv, 967 pp.

Oldfield RC (1971): The assessment and analysis of handedness: The Edinburgh inventory. Neuropsychologia 9:97–113.

Pagani E, Filippi M, Rocca MA, Horsfield MA (2005): A method for obtaining tract-specific diffusion tensor MRI measurements in the presence of disease: Application to patients with clinically isolated syndromes suggestive of multiple sclerosis. Neuroimage 26:258–265.

Pagani E, Hirsch JG, Pouwels PJ, Horsfield MA, Perego E, Gass A, Roosendaal SD, Barkhof F, Agosta F, Rovaris M, Caputo D, Giorgio A, Palace J, Marino S, De Stefano N, Ropele S, Fazekas F, Filippi M (2010): Intercenter differences in diffusion tensor MRI acquisition. J Magn Reson Imaging 31:1458–1468.

Parisi L, Rocca MA, Valsasina P, Panicari L, Mattioli F, Filippi M (2014): Cognitive rehabilitation correlates with the functional connectivity of the anterior cingulate cortex in patients with multiple sclerosis. Brain Imaging Behav 8:387–393.

Patenaude B, Smith SM, Kennedy DN, Jenkinson M (2011): A Bayesian model of shape and appearance for subcortical brain segmentation. Neuroimage 56:907–922.

Philp DJ, Korgaonkar MS, Grieve SM (2014): Thalamic volume and thalamo-cortical white matter tracts correlate with motor and verbal memory performance. Neuroimage 91:77–83.

Polman CH, Reingold SC, Banwell B, Clanet M, Cohen JA, Filippi M, Fujihara K, Havrdova E, Hutchinson M, Kappos L, Lublin FD, Montalban X, O'Connor P, Sandberg-Wollheim M, Thompson AJ, Waubant E, Weinshenker B, Wolinsky JS (2011): Diagnostic criteria for multiple sclerosis: 2010 revisions to the McDonald criteria. Ann Neurol 69:292–302.

Poonawalla AH, Hasan KM, Gupta RK, Ahn CW, Nelson F, Wolinsky JS, Narayana PA (2008): Diffusion-tensor MR imaging of cortical lesions in multiple sclerosis: initial findings. Radiology 246:880–886.

Portaccio E, Goretti B, Zipoli V, Siracusa G, Sorbi S, Amato MP (2009): A short version of Rao's Brief Repeatable Battery as a screening tool for cognitive impairment in multiple sclerosis. Clin Neuropsychol 23:268–275.

Rao SM, Leo GJ, Bernardin L, Unverzagt F (1991): Cognitive dysfunction in multiple sclerosis. I. Frequency, patterns, and prediction. Neurology 41:685–691.

Reese TG, Heid O, Weisskoff RM, Wedeen VJ (2003): Reduction of eddy-current-induced distortion in diffusion MRI using a twice-refocused spin echo. Magn Reson Med 49:177–182.

Rocca MA, Valsasina P, Hulst HE, Abdel-Aziz K, Enzinger C, Gallo A, Pareto D, Riccitelli G, Muhlert N, Ciccarelli O, Barkhof F, Fazekas F, Tedeschi G, Arévalo MJ, Filippi M; MAGNIMS fMRI Study Group (2014): Functional correlates of cognitive dysfunction in multiple sclerosis: A multicenter fMRI Study. Hum Brain Mapp 35:5799–5814.

Sepulcre J, Sastre-Garriga J, Cercignani M, Ingle GT, Miller DH, Thompson AJ (2006): Regional gray matter atrophy in early primary progressive multiple sclerosis: A voxel-based morphometry study. Arch Neurol 63:1175–1180.

Smith SM (2002): Fast robust automated brain extraction. Hum Brain Mapp 17:143–155.

Smith SM, Zhang Y, Jenkinson M, Chen J, Matthews PM, Federico A, De Stefano N (2002): Accurate, robust, and automated longitudinal and cross-sectional brain change analysis. Neuroimage 17:479–489.

Stejskal EO (1965): Use of spin echoes in a pulsed magnetic-field gradient to study anisotropic, restricted diffusion and flow. J Chem Phys 43:3597–3603.

Till C, Ghassemi R, Aubert-Broche B, Kerbrat A, Collins DL, Narayanan S, Arnold DL, Desrocher M, Sled JG, Banwell BL (2011): MRI correlates of cognitive impairment in childhood-onset multiple sclerosis. Neuropsychology 25:319–332.

Tona F, Petsas N, Sbardella E, Prosperini L, Carmellini M, Pozzilli C, Pantano P (2014): Multiple sclerosis: Altered thalamic resting-state functional connectivity and its effect on cognitive function. Radiology 271:814–821.

Tovar-Moll F, Evangelou IE, Chiu AW, Richert ND, Ostuni JL, Ohayon JM, Auh S, Ehrmantraut M, Talagala SL, McFarland HF, Bagnato F (2009): Thalamic involvement and its impact on clinical disability in patients with multiple sclerosis: A diffusion tensor imaging study at 3T. AJNR Am J Neuroradiol 30:1380–1386.

Traynor C, Heckemann RA, Hammers A, O'Muircheartaigh J, Crum WR, Barker GJ, Richardson MP (2010): Reproducibility of thalamic segmentation based on probabilistic tractography. Neuroimage 52:69–85.

van Asselen M, Kessels RP, Neggers SF, Kappelle LJ, Frijns CJ, Postma A (2006): Brain areas involved in spatial working memory. Neuropsychologia 44:1185–1194.

Watkins KE, Paus T, Lerch JP, Zijdenbos A, Collins DL, Neelin P, Taylor J, Worsley KJ, Evans AC (2001): Structural asymmetries in the human brain: A voxel-based statistical analysis of 142 MRI scans. Cereb Cortex 11:868–877.

Whelan R, Lonergan R, Kiiski H, Nolan H, Kinsella K, Hutchinson M, Tubridy N, Reilly RB (2010): Impaired information processing speed and attention allocation in multiple sclerosis patients versus controls: A high-density EEG study. J Neurol Sci 293:45–50.

Yu HJ, Christodoulou C, Bhise V, Greenblatt D, Patel Y, Serafin D, Maletic-Savatic M, Krupp LB, Wagshul ME (2012): Multiple white matter tract abnormalities underlie cognitive impairment in RRMS. Neuroimage 59:3713–3722.